# Distribution and texture of platinum group minerals in the C and West Cave zones of the New Afton Cu-Au deposit, British Columbia

Wyatt Bain[1, a], Robin Joudrie[1], Freia de Waal[2], Mitchell G. Mihalynuk[3], and Dylan Goudie[4]

[1] Department of Earth Sciences, University of Western Ontario, London, ON, N6A 3K7
[2] University of Victoria, Victoria, BC, V8P 5C2
[3] British Columbia Geological Survey, Ministry of Mining and Critical Minerals, Victoria, BC, V8W 9N3
[4] Core Research Equipment and Instrument Training (CREAIT) Network, Memorial University of Newfoundland, St. John's, NL, A1C 5S7
[a] corresponding author: wbain2@uwo.ca

Recommended citation: Bain, W., Joudrie, R., de Waal, F., Mihalynuk, M.G., and Goudie, D., 2026. Distribution and texture of platinum group minerals in the C and West Cave zones of the New Afton Cu-Au deposit, British Columbia. In: Geological Fieldwork 2025, British Columbia Ministry of Mining and Critical Minerals, British Columbia Geological Survey Paper 2026-01, pp. 85-95.

**Abstract**

Alkalic Cu-Au porphyry deposits in the Quesnel terrane of British Columbia represent an important source of Cu-Au and commonly contain byproduct platinum group elements (PGE) and discrete platinum group minerals (PGM). Several studies have evaluated the occurrence of PGM in alkalic porphyries in British Columbia, but the occurrence of PGM and the processes that drive PGE enrichment in this setting remain incompletely understood. This study evaluates the paragenesis and mineral associations of PGM in the C and West Cave zones of the New Afton deposit, using quantitative scanning electron microscopy-mineral liberation analysis (SEM-MLA). PGM occur in ore-stage mineralization from most underground zones (e.g., C, West Cave, and East Extension) with the C and West Cave zones having the highest relative abundances identified to date. The textures and mineral association of PGM of the C and West Cave zones indicate that they crystallized throughout the paragenesis of these areas and are intergrown with the primary mineralogy of Fe oxide-apatite veins, Fe oxide-sulphide veins, sulphide veins, zones of disseminated sulphides, and late-stage carbonate veins. Occurrences of PGM grains suggest contemporaneity with intense potassic and sodic-potassic alteration, and PGM grains commonly co-occur with grains of electrum, tetrahedrite, and Ag-Hg tellurides. The distribution of PGM in hypogene Cu-Au mineralization and late carbonate-bearing veins suggests the New Afton deposit had multi-stage PGE enrichment and mobilization in the presence of magmatic fluids.

**Keywords:** Alkalic porphyry Cu-Au, New Afton, critical minerals, platinum group elements, cobalt, nickel

## 1. Introduction

Canada (NRCan, 2024) and many of its trading partners identify platinum group elements (PGEs) as critical minerals (e.g., Table 1 in Hickin et al., 2024). PGEs are among the rarest elements in the Earth's crust, typically having concentrations of <0.6 ppb (Rudnick and Gao, 2014). Deposits featuring high concentrations of these metals are relatively rare. Most of the world's PGE supply is produced as a byproduct or co-product of Ni and Cu refining outside of North America (Gunn, 2014). As the need for PGEs grows, so too will the need for secure supply chains, including potential domestic PGE sources (NRCan, 2024).

With the closure of Canada's only primary PGE-producing mine (Lac-des-Iles, Ontario) in 2026, domestic PGE production in Canada will be primarily as a byproduct of nickel production from magmatic sulphide deposits in eastern Canada. However, ore concentrates from several 'alkalic' porphyry Cu-Au-Ag±Mo deposits (Barr et al., 1976) in British Columbia contain significant concentrations of PGEs (Nixon and Laflamme, 2002) that might support additional domestic PGE production.

Quesnel and Stikine terranes (Fig. 1) contain one of the largest concentrations of alkalic porphyry Cu-Au-Ag±Mo deposits in the world (Logan and Mihalynuk, 2014). In addition to primary Cu-Au±Ag production, these deposits contain significant PGE, Te, Re, Co, and Bi (Hofstra and Kreiner, 2020). Recent work on alkalic porphyry deposits such as New Afton and Kwanika (Fig. 2a) shows that PGEs commonly occur in high abundances with primary Cu-Au minerals, and in some cases are concentrated in PGE-rich minerals (Hofstra and Kreiner, 2020; Boucher et al., 2023; Robb et al., 2023; Karatas Ahmadli, 2025; Polar, 2025). Reliable prediction of PGE grade and production requires detailed knowledge of PGE mineralogy (Bissig and Cooke, 2014).

The New Afton alkalic deposit in south-central British Columbia is primarily a Cu-Au-Ag porphyry. However, ore from this deposit commonly has elevated concentrations of PGEs (Pd >1 ppm) and hosts platinum group minerals (PGMs; discrete Pd-Pt-Sb-As-Te-Hg-Bi mineral phases in which PGEs are a major constituent by weight; Boucher et al., 2023; Robb et al., 2023). Limited metallurgical testing

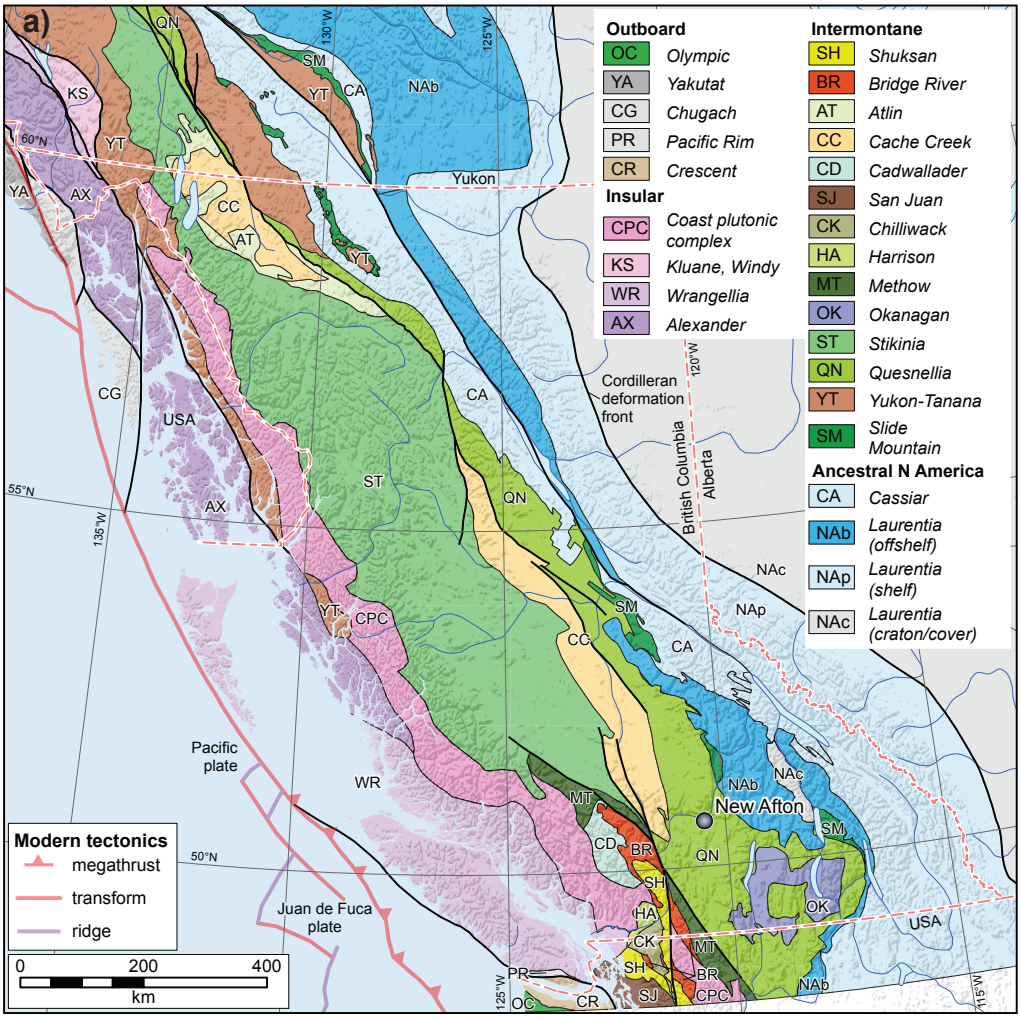


**Fig. 1. a)** Location of the New Afton deposit in British Columbia. Terranes modified from Colpron (2020). **b)** Locations of alkalic porphyry deposits in Quesnel and Stikine terranes and the location of the Iron Mask batholith; modified after Logan and Mihalynuk (2014).

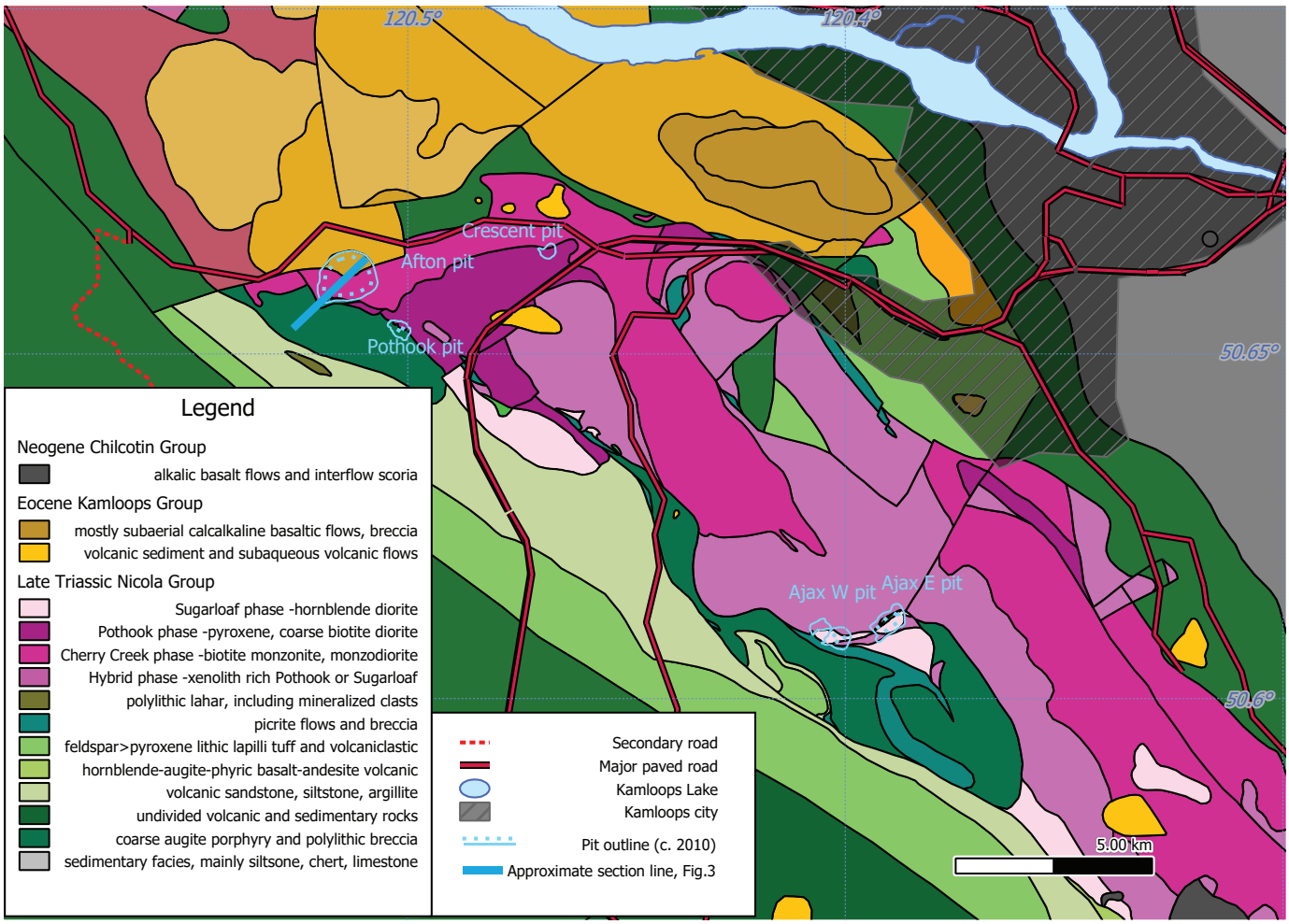


**Fig. 2.** Geologic map showing the location of the New Afton deposit and other porphyry deposits in the Iron Mask batholith. Modified after Logan et al. (2006) and Diakow and Mihalynuk (unpublished).

in 2024 produced an ore concentrate containing 62% copper with 2.95 g/t of recoverable Pd (Parson et al., 2024). In this paper, we report on the mineralogical and textural features of rock types with anomalous PGE contents, and on microscale mineral affinities and distributions of PGM in the New Afton underground deposit. We highlight the occurrence of PGM throughout the paragenesis of mineralization and importantly, in secondary mineralization not typically targeted for production at New Afton, such as Fe oxide veins, Fe oxide-apatite veins, and late-stage carbonate veins.

## 2. Alkalic porphyry deposits

Porphyry deposits are low-grade high tonnage magmatic-hydrothermal deposits that can be subdivided into calc-alkalic and alkalic varieties based on the composition of causative intrusions (Cooke et al., 2005; Sillitoe, 2010). In British Columbia, alkalic Cu-Au porphyry deposits occur mainly in arc settings (e.g., Logan and Mihalynuk, 2014) and are classically associated with silica-undersaturated to saturated intrusive rocks (Barr et al., 1976; Sillitoe, 2010). A distinctive feature of alkalic porphyries is their discrete, magnetite-rich alteration footprints. These footprints commonly comprise a high-temperature potassic (biotite-K-feldspar-magnetite), calc-potassic (epidote-magnetite-actinolite-K-feldspar±garnet-apatite), or calc-sodic (albite-epidote±diopside) cores surrounded by zones of sericite-anhydrite-carbonate and propylitic alteration (Lang et al., 1995a, b; Polar, 2025). High-grade mineralization in alkalic porphyry deposits is most commonly associated with potassic and calc-potassic alteration (Cooke et al., 2007; Polar, 2025).

A number of studies have highlighted elevated PGE concentrations in alkalic porphyry deposits and alkaline igneous complexes in British Columbia (Fig. 1b), including Mt. Polley (Pass et al., 2009; Pass, 2010), Galore Creek (Lang et al., 1995b; Thompson et al., 2002), Lorraine (Nixon, 2003a; Nixon and Peatfield, 2003), Mt. Milligan (LeFort et al., 2011), Kwanika (Karatas Ahmadli, 2025), Ajax East, New Afton (Nixon, 2003b; Hanley et al., 2020; Robb et al., 2023; Boucher et al., 2023), and the Whiterocks Mountain and Sappho alkaline complex (Nixon, 2001, 2002; Nixon and Carbno, 2001; Nixon and Archibald, 2002). Thompson et al. (2002) examined heavy mineral concentrates from Galore Creek, Lorraine, Mt. Milligan, Mt. Polley, and Ajax East and noted that high PGE values were associated

with a mixture of sulphides (bornite, chalcopyrite, and pyrite) and oxides (magnetite and hematite), suggesting that the PGE-bearing mineral phases were part of ore-stage sulphide-oxide mineralization. Additional work by Robb et al. (2023), Boucher et al. (2023), and Karatas Ahmadli (2025) examined the distribution of PGEs in the New Afton and Kwanika deposits and further showed that high PGE values correlate with PGE-bearing mineral phases.

## 3. The New Afton deposit

The New Afton deposit (Late Triassic; 204.5 ±0.6 to 201.39 ±0.75 Ma; U-Pb zircon; Logan et al., 2007; Logan and Mihalynuk, 2014) is one of several centres of alkalic porphyry mineralization in the southern Quesnel terrane related to the Iron Mask batholith (Logan and Mihalynuk, 2005; Logan et al., 2006, 2007; Lipske et al., 2020, 2021). The southern portion of the Quesnel terrane is predominantly a Late Triassic volcanic arc, comprising volcanic and volcanosedimentary rocks (Nicola Group) and allied plutonic rocks (Logan et al., 2007; Mihalynuk et al., 2016; Mihalynuk and Diakow, 2020).

At the New Afton deposit (Figs. 2, 3) mineralization is spatially associated with porphyritic monzonite rocks that intrude Nicola Group, andesitic to picritic basalt flows, breccias, and tuffs (Hall and May, 2013; Lipske et al., 2020). The Cu-Au mineralization comprises chalcopyrite±bornite, lesser chalcocite-covellite, and sulphosalts that occur in veinlets, breccias, and disseminated sulphides within potassic, calc-potassic, and calc-sodic alteration zones, primarily in Nicola Group volcanic rocks, monzodiorite and, to a lesser extent, diorite intrusions (e.g., Polar, 2025). The mineralization is structurally controlled, with steep north-trending extensional structures interpreted as the principal conduits for emplacement of both magmas and magmatic-hydrothermal fluids (e.g., Hall and May, 2013; Polar, 2025).

Mineralized zones in the New Afton deposit contain elevated Pd and variably elevated Pt; Pd-Pt occurs in association with pyrite and chalcopyrite and with Pd-Pt-Sb-As-Te-Hg ±Bi PGM (temagamite, isomertieite, mertieite, cooperite, naldrettite, sperrylite, moncheite, and kotulskite). Boucher et al. (2023) showed that high PGE concentrations are associated with Co-Ni-bearing pyrite having growth zones defined by variations in PGE concentrations. Similarly, Robb et al. (2023) noted that PGM are most common in areas where whole-rock assays for Pd+Pt are >1 ppm and typically with elevated Au grades.

Although magnetite enrichment is common in alkalic deposits, Fe oxide-apatite veins are not. At the New Afton deposit, Fe oxide-apatite veins are a characteristic feature (Polar, 2025 and referenced therein) and appear to have an association with Cu-Au and PGE-enrichment that is not well understood.

## 4. Methods

### 4.1. Sample selection

Samples used in this study were collected during the summer of 2024, targeting high-PGE grade intersections in drill core cut between 2006 and 2022. Sample selection focused on

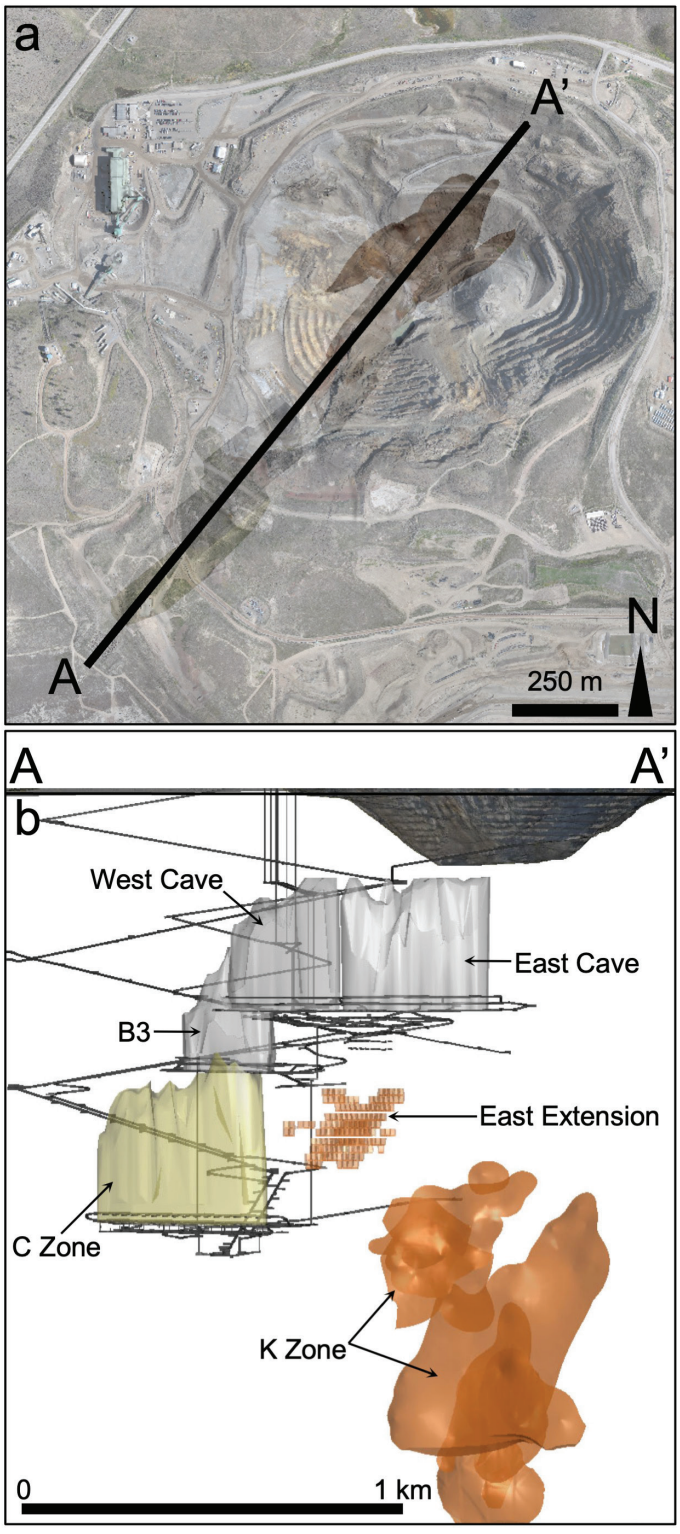


**Fig. 3. a)** Satellite image of the New Afton open pit showing the section line for b). **b)** Schematic 3D cross-section of the New Afton open pit showing the location of ore zones. Grey shapes (East Cave, West Cave, B3) denote volumes that have already been mined. The gold shape (C zone) denotes a volume currently under production. The orange shapes denote unmined parts of the deposit. No vertical exaggeration. Images courtesy of New Gold Inc.

zones with correlated elevations of Co, Ni, and PGE contents, typically where 2 m assay intervals returned >100 ppm Co, >100 ppm Ni, or >0.1 ppm $PGE_{tot}$, or on intervals displaying characteristic alteration and mineralization styles. Core samples were typically 10-20 cm long intervals halved into subsamples for analysis and archiving. A total of 38 samples were selected from the C, West Cave, East Cave, East Extension, B3, and K zones (Fig. 3b) for SEM-MLA analysis. We focus here on samples from the West Cave and C zones.

### 4.2. Scanning electron microscopy-mineral liberation analysis (SEM-MLA)

Quantitative mineral studies were conducted at Memorial University of Newfoundland's CREAIT Microanalysis Facility using a FEI Quanta field emission gun 650 scanning electron microscope (SEM) equipped with mineral liberation analysis (MLA) software version 3.14 (Sylvester, 2012; Grant et al., 2018; Beranek et al., 2023). Instrument conditions included a 25 kV accelerating voltage, 13.5 mm working distance, and 10 nA beam current. The MLA frames were 1.5 by 1.5 mm with a resolution of 500 by 500 pixels. Backscatter electron (BSE) images of each frame were used to identify features based on the contrast in the BSE signal across mineral grain boundaries. Features were identified at a baseline resolution of 30 µm, or less in cases where adjacent mineral grains had dramatically different contrast in BSE images. MLA maps were created using GXMAP mode by acquiring energy-dispersive X-ray spectra at a grid spacing of 10 pixels, with a spectral dwell time of 12 ms, and comparing them against an in-house library of mineral reference spectra. The accuracy of mineral identification was verified using in situ imaging and point analysis in the CREAIT Microanalysis Facility during SEM-MLA data collection. MLA images were then processed in Adobe® Photoshop® to highlight various features, such as mineralogical contrast, crosscutting relationships, and key mineral phases.

## 5. Results

Platinum group minerals were detected in samples from the C (n=7), West Cave (n=4), and East Extension (n=3) zones and comprise discrete Pd-Pt-Sb-As-Bi mineral phases. In all cases, PGM are closely associated with electrum and tetrahedrite (Fig. 4; Figs. 5a, d), and in most cases, Ag-Hg tellurides. Samples lacking PGM, including those from the B3, East Cave, and K zones, typically contained abundant electrum and tetrahedrite, with variable Ag-Hg tellurides, but were not evaluated further in this study. The highest PGM abundances (on the basis of particle count and area % per sample) are in samples from the West Cave and C zones.

### 5.1. PGE minerals in C zone samples

PGM in the C zone are associated with disseminated sulphides, sulphide-carbonate±quartz veins, Fe oxide-sulphide veins, and Fe oxide-apatite veins. PGM are most abundant in samples of specular hematite-rich Fe oxide-sulphide veins (Fig. 5) and Fe oxide-apatite veins (Fig. 6).

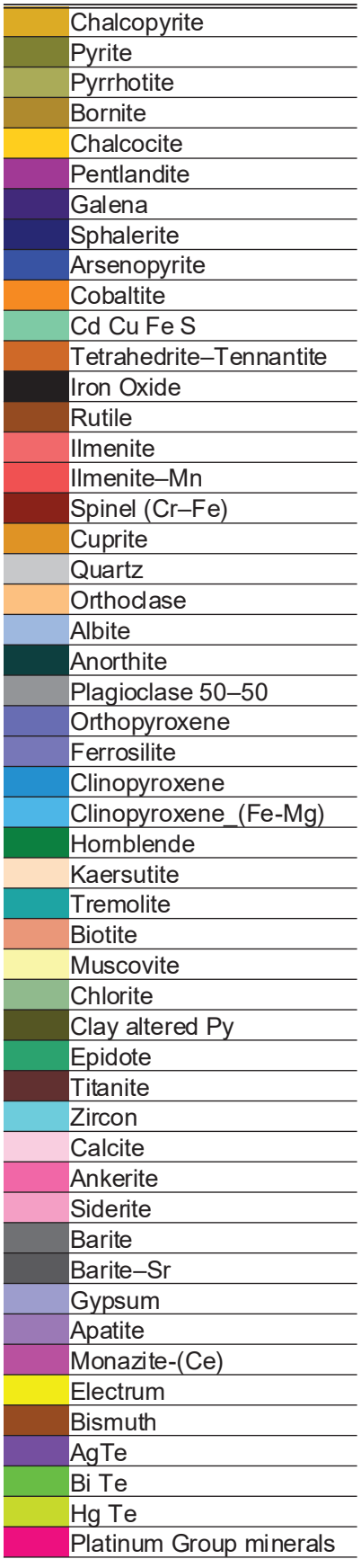


**Fig. 4.** Legend for the colour SEM-MLA maps in Figures 5-10.

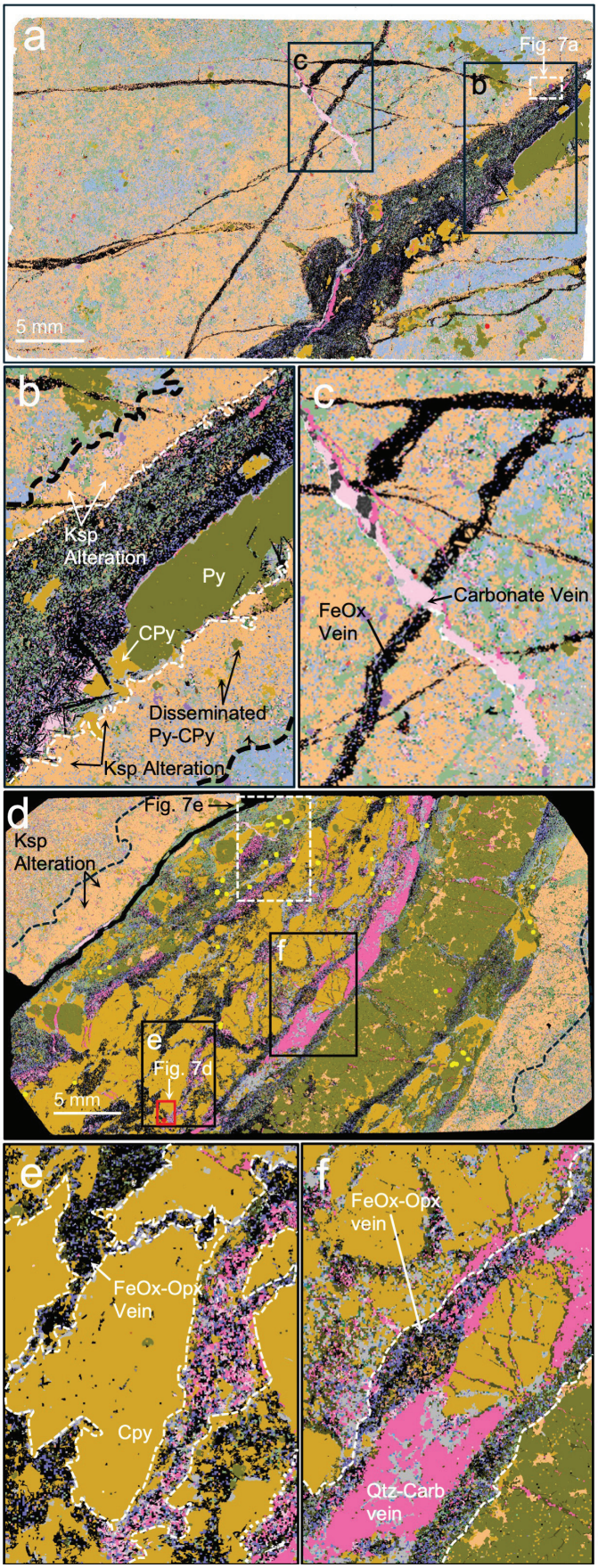


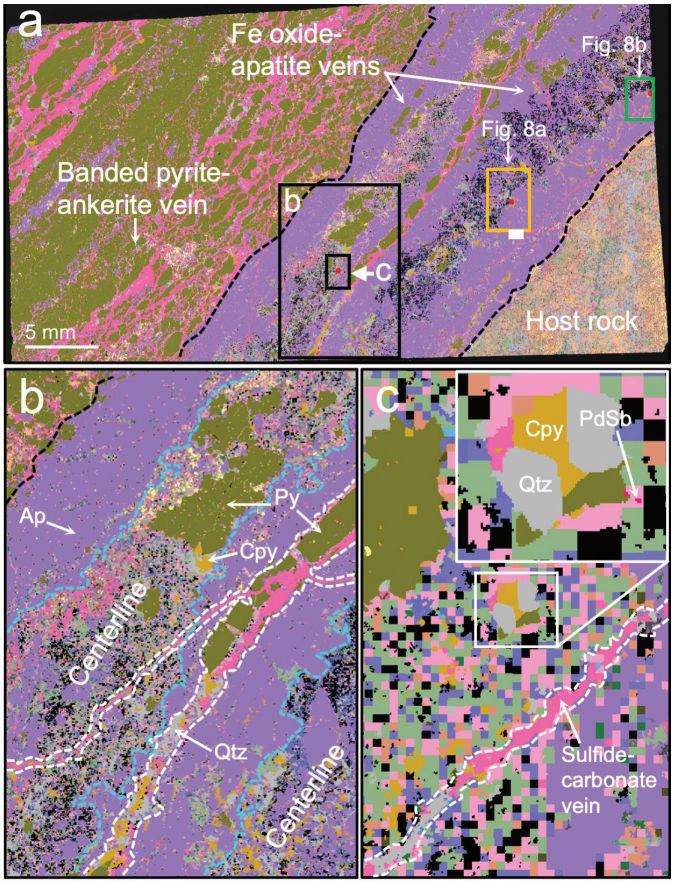


**Fig. 6. a)** Colour maps of sample 206-18G showing an Fe oxide-apatite vein from the C zone. The inset image in Figure 8a is outlined in orange. The inset image shown in Figure 8b is outlined in green. Red dots denote the location of PGM grains. **b)** Inset image showing the centreline of an Fe oxide-apatite vein and a subparallel, crosscutting sulphide-carbonate vein. **c)** Inset image showing the location of intergrown calcite, quartz (Qtz), pyrite (Py), and chalcopyrite (CPy) hosting a grain of PdSb in the centreline mineralogy.

**Fig. 5.** Colour maps of selected samples from the C zone. **a)** Colour map of sample 206-18M showing a sulphide-poor Fe oxide-sulphide vein. The area shown in Figure 7a is outlined with a white dashed line. **b)** Inset image showing the edges of the Fe oxide-sulphide vein (outlined with a dashed white line), the outer edge of the potassic (Ksp) alteration halo (outlined with a black dashed line) and disseminated pyrite (Py) and chalcopyrite (CPy). **c)** Secondary carbonate veins crosscutting earlier Fe-oxide veins. **d)** Colour maps of sample 206-18N showing a sulphide-rich Fe oxide-sulphide vein. Red dot denotes the location of PGM grains. Yellow dots denote the location of electrum grains. The area shown in Figure 7d, is outlined in red. The area shown in Figure 7e, is outlined with a white dashed line. **e, f)** Inset images showing banding of coarse sulphides and the fine-grained intergranular gauge mineralogy. Note the later-stage carbonate-sulphide vein (outlined with a white dashed line) crosscutting the earlier sulphides in f).

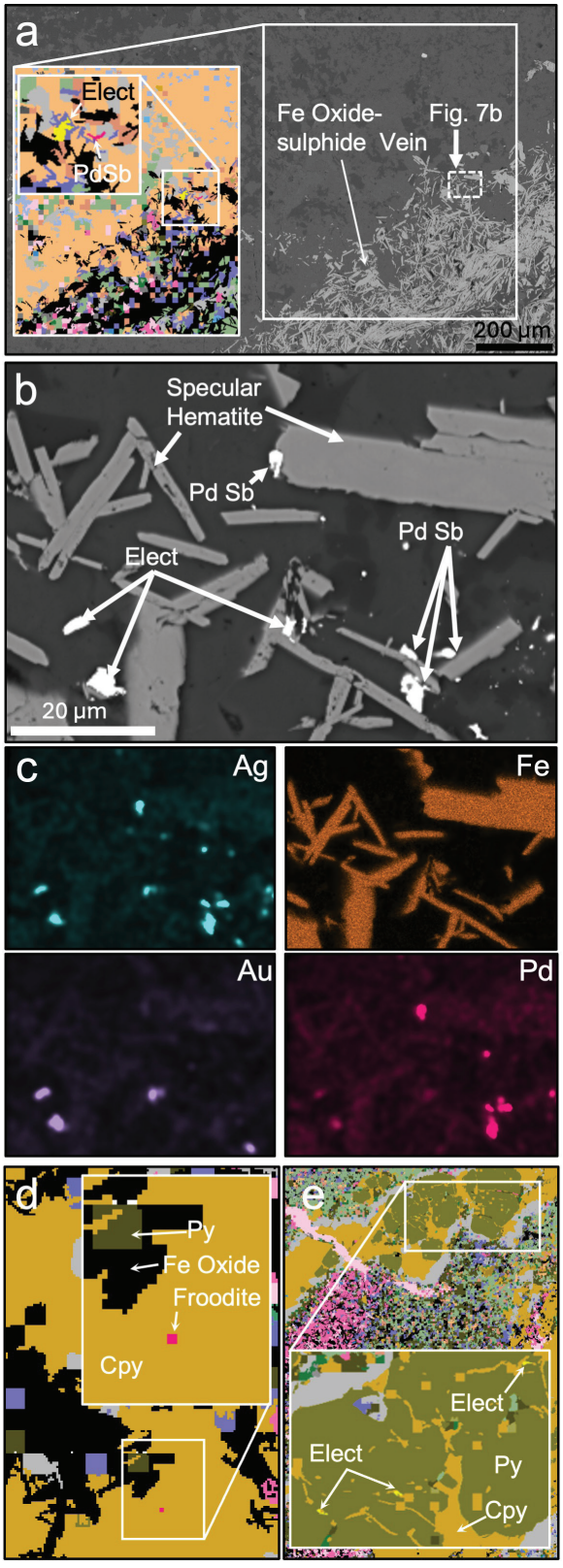


**Fig. 7. a)** BSE image with MLA inset image showing electrum and PdSb along the edge of the sulphide-poor Fe oxide (FeOx)-sulphide vein shown in Figure 5a. **b, c)** Close-up BSE image and corresponding EDS maps showing intergrown PdSb, electrum (Elect), and specular hematite. **d, e)** Inset images outlined on Figure 5d showing a froodite grain and electrum hosted in chalcopyrite.

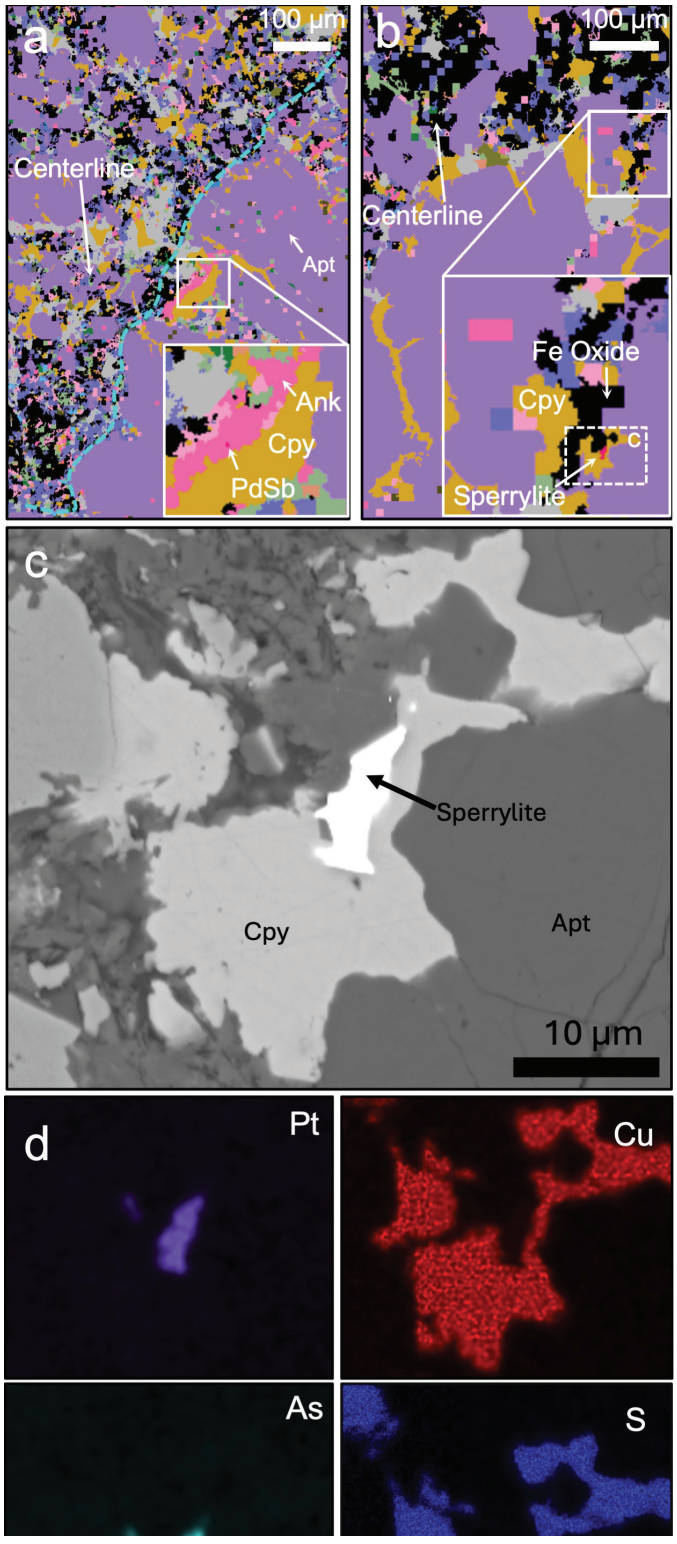


**Fig. 8.** Images of outlined areas shown in Figure 6a. **a)** Carbonate- and **b)** Chalcopyrite-hosted PdSb and sperrylite in the centreline of a comb-textured Fe oxide-apatite vein. **c)** Close-up BSE image and **d)** Corresponding EDS maps of the chalcopyrite-hosted sperrylite grain shown in b). Area of panels in d) is the same as that shown in c). Ap=apatite; Ank=ankerite.

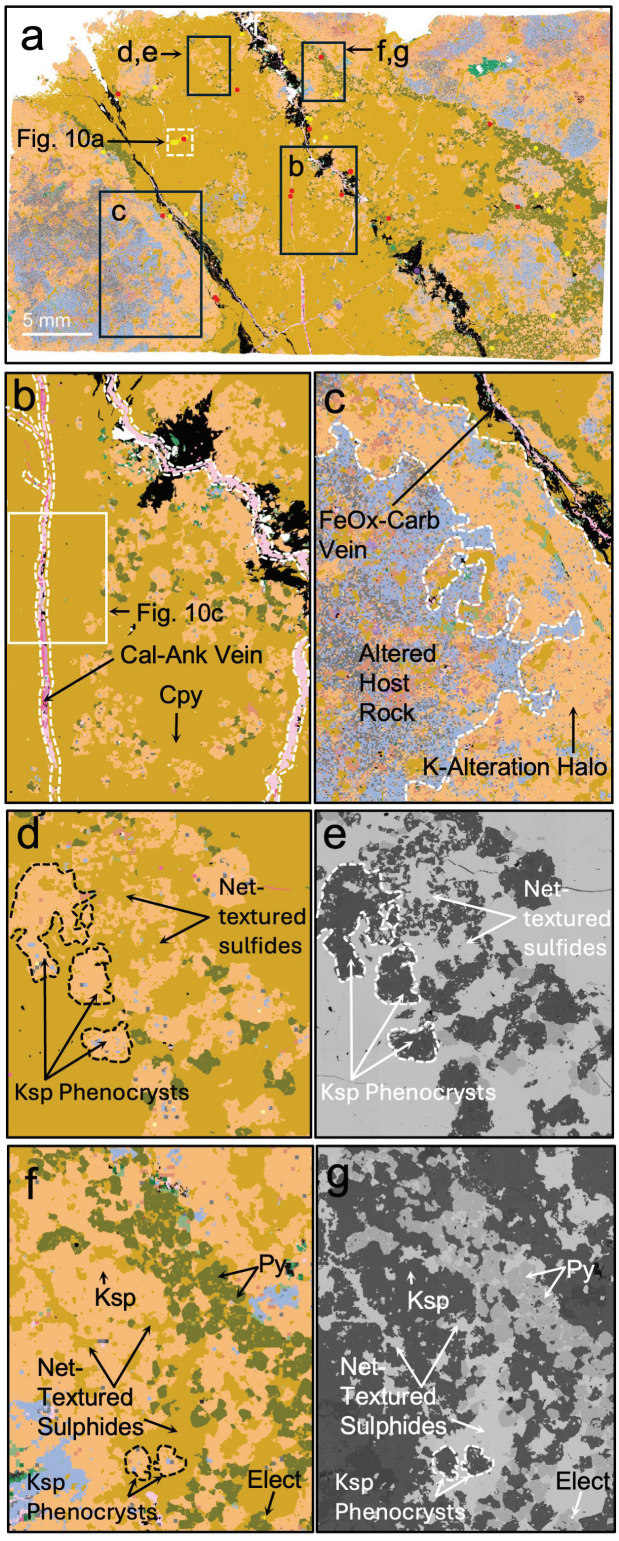


**Fig. 9. a)** Colour maps of a sulphide vein from the West Cave zone (Sample 210-34J). Red dots denote the location of PGM grains. Yellow dots denote the location of electrum grains. The white dashed square indicates the location of Figure 10a. **b)** Inset image showing calcite-ankerite (Cal-Ank) veins crosscutting primary chalcopyrite. White rectangle indicates location of Figure 10c. **c)** Inset image showing the intense potassic (K) alteration halo along the edges of the sulphide vein. **d, f)** Colour maps and corresponding BSE images **e, g)** of net-textured chalcopyrite surrounding euhedral orthoclase crystals.

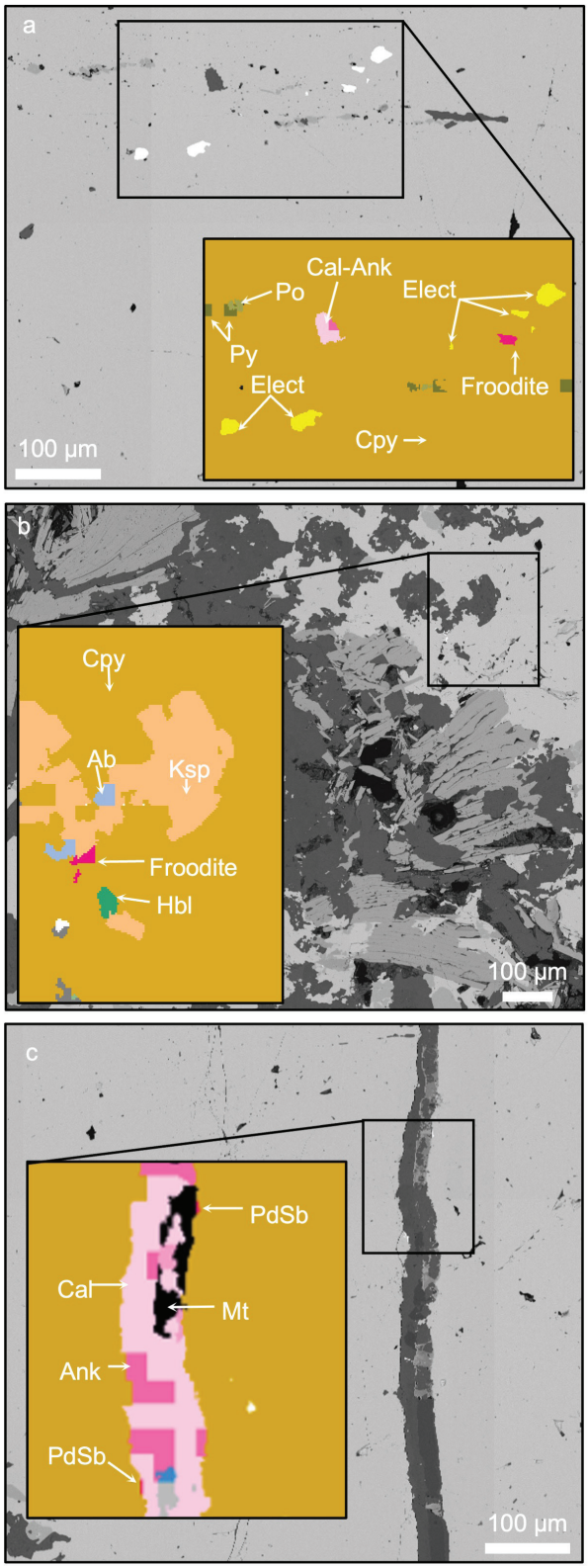


**Fig. 10. a)** BSE image with MLA inset image showing electrum and froodite grains in chalcopyrite. See Figure 9a for context. **b)** BSE image with MLA inset image showing a froodite grain associated with net-textured chalcopyrite. See Figure 9c for context **c)** Secondary calcite-ankerite (Cal-Ank) vein with PbSb grains along its margins. See Figure 9b for context. Mt=Magnetite; Ab=Albite; Hbl=hornblende; Ksp=orthoclase.

#### 5.1.1. Specular hematite-rich Fe oxide-sulphide veins

In the C zone, PGM-bearing specular hematite-rich Fe oxide-sulphide veins commonly crosscut sodic-potassic-altered host rock and are surrounded by halos of intense potassic alteration with variable concentrations of disseminated pyrite and chalcopyrite (Figs. 5b, c, d). The veins range in composition and texture from predominantly specular hematite with subordinate pyrite-chalcopyrite and intergranular carbonate-magnetite-epidote-feldspar-quartz-pyroxene (i.e., sulphide-poor; Figs. 5a, c), to predominantly pyrite-chalcopyrite surrounded by fine-grained Fe oxide-carbonate-epidote-feldspar-quartz-pyroxene (i.e., sulphide-rich; Figs. 5d-f). In both cases, the sulphide minerals are typically concentrated along vein margins (Fig. 5b) or cores (Figs. 5d-f). Commonly, the most sulphide-rich veins have a banded appearance and are composed of multiple, parallel sets of veins (Figs. 5d, 6). Both the sulphide-poor and sulphide-rich veins are crosscut by carbonate-quartz-sulphide veins (Figs. 5c, 6b).

PGE minerals in sulphide-poor veins include PdSb alloy and froodite ($PdBi_2$). Pb-Sb alloy is commonly found together with electrum and intergrown with specular hematite and fine-grained silicates along vein margins (Fig. 7) or in the disseminated pyrite. Froodite is accompanied by electrum and occurs as crystals intergrown with chalcopyrite in sulphide-rich veins (Figs. 7d, e). PGM in sulphide-poor and sulphide-rich Fe oxide-sulphide veins from the East Extension zone display similar textures and mineral associations but are hosted in veins with more intense sodic-calcic alteration.

#### 5.1.2. Fe oxide-apatite veins

PGM-bearing Fe oxide-apatite veins sampled from the C zone contain comb-textured apatite at vein margins with vein centrelines composed of fine-grained Fe oxide-carbonate-quartz-pyroxene-epidote-chlorite-sulphide (Fig. 6). Sulphide in this setting ranges in texture and composition from pyrite to fine-grained intergranular chalcopyrite (Figs. 6b, c). The Fe oxide-apatite veins are commonly part of larger banded sulphide veins, as seen in Figure 6a where two parallel Fe oxide-apatite veins are bound on one side by sodic-potassic altered host rock and on the other by a parallel banded pyrite-ankerite vein (Fig. 6b). The two Fe oxide-apatite veins in this instance are separated by and crosscut by a parallel pyrite-ankerite veinlet of ankerite.

PGM associated with Fe oxide-apatite veins include PdSb alloy and sperrylite ($PtAs_2$; Figs. 8c, d) intergrown with chalcopyrite, carbonate, and Fe oxide along the centrelines of the veins (e.g., Fig. 6c; Figs. 8a, b). PGM in this setting. PGE minerals in Fe oxide-apatite veins from the East Extension zone display similar textures and mineral associations.

### 5.2. PGE minerals in West Cave zone samples

PGM are present in four samples from the West Cave zone. In this zone, they are predominantly hosted in sulphide veins (e.g., Figs. 9, 10) and in disseminated sulphides within host rocks, which are overprinted by intense sodic-potassic and potassic alteration. Sparse PGM are also present in Fe oxide-sulphide and Fe oxide-apatite veins.

#### 5.2.1. Sulphide veins

PGM-bearing sulphide veins display intense halos of potassic alteration where they crosscut sodic-potassic altered host rocks. They are, in turn, cut by carbonate and carbonate-Fe oxide-filled fractures (Figs. 9a-c). Sulphide veins contain massive chalcopyrite with abundant pyrite along the vein margins. In the veins, chalcopyrite surrounds K-feldspar crystals and exhibits a net-textured appearance (Figs. 9d-g). Chalcopyrite veins in the C zone have a similar net-textured appearance and contain electrum.

PGM observed in sulphide veins include PdSb alloy and froodite (Fig. 10). Froodite most commonly occurs with chalcopyrite, electrum, and orthoclase displaying net-textured sulphides (Figs. 10a, b). PdSb alloy most commonly occurs along the margins of carbonate-Fe oxide-filled fractures where they crosscut earlier chalcopyrite veins (Fig. 10c).

## 6. Discussion

PGM in the C and West Cave zones are hosted by early Fe oxide-apatite veins, ore-stage Fe oxide-sulphide veins, and late-stage carbonate veins. This suggests PGE mobilization, enrichment, and deposition under variable oxidation and sulfidation conditions at multiple times during the formation of the New Afton deposit.

The mineralogic and textural associations of PGM described in this paper are consistent with those presented by Robb et al. (2023) and Boucher et al. (2023) and with observations of PGE mineralization in other alkalic porphyry deposits in British Columbia (Pass, 2010; LeFort et al., 2011), including nearby deposits also within the Iron Mask batholith (Nixon and Leflamme, 2002; Nixon, 2003b; MacKenzie, 2009). In their study of PGE mineralization in the New Afton deposit, Robb et al. (2023) and Boucher et al. (2023) concluded that PGE enrichment in sulphides occurred during the formation of early- and main-stage hypogene mineralization via discrete pulses of high-temperature magmatic fluids and under conditions of fluctuating temperature, $fO_2$, and $fS_2$. PGM abundances increased during remobilization of PGEs from hypogene sulphides during secondary hydrothermal processes involving the formation of carbonate-rich, oxidized alteration assemblages (Robb et al., 2023; Boucher et al., 2023). Observations presented here, including PGM in hypogene Cu-Au mineralization and late-stage carbonate veins, are consistent with those presented by Robb et al. (2023) and Boucher et al. (2023) and likely reflect a similar model of fluid evolution and deposit formation.

## 7. Conclusion

This study and previous studies examining PGE enrichment in deposits like New Afton highlight that critical metals such as PGEs, Co, and Te, can occur as potentially economic byproducts on the deposit scale but be overlooked during exploration and

processing. Our study demonstrates the utility of quantitative SEM-MLA in rapidly recognizing and characterizing subtle mineralogic features associated with enrichment of PGEs.

**Acknowledgments**

We thank Dr. Evan Orovan (Thesis Gold), Dr. Stephen Piercey (Memorial University), Sean Tombe and Devin Wade (New Gold) for their reviews, which substantially improved this paper. We also thank Sean Tombe and Devin Wade for their help with accessing the drill core and arranging fieldwork at the New Afton deposit. Kaitlyn McLaren (BCGS) provided geographic information system support.

**References cited**

Bain, W.M., de Waal, F., and Goudie, D.J., 2025. Co-Te mineralization in iron skarns on Vancouver Island and Texada Island. In: Geological Fieldwork 2024, British Columbia Ministry of Mining and Critical Minerals, British Columbia Geological Survey Paper 2025-01, pp. 153-175.

Barr, D.A., Fox, P.E., Northcote, K.E., and Preto, V.A., 1976. The alkaline suite porphyry deposits: A summary. In: Sutherland Brown, A., (Ed.), Porphyry Deposits of the Canadian Cordillera. Canadian Institute of Mining and Metallurgy, Special Volume 15, pp. 359-367.

Beranek, L.P., Hutter, A.D., Pearcey, S., James, C., Langor, V., Pike, C., Goudie, D., and Oldham, L., 2023. New evidence for the Baltican cratonic affinity and Tonian to Ediacaran tectonic evolution of West Avalonia in the Avalon Peninsula, Newfoundland, Canada. Precambrian Research, 390. <https://doi.org/10.1016/j.precamres.2023.107046>

Bissig, T., and Cooke, D.R., 2014. Introduction to the Special Issue devoted to alkalic porphyry Cu-Au and epithermal Au deposits. Economic Geology, 109, 819-825. <https://doi.org/10.2113/econgeo.109.4.819>

Boucher, B.M., Robb, S.J., Hanley, J.J., Kerr, M.J., and Mungall, J.E., 2023. Platinum-group elements (PGE) in the New Afton alkalic Cu-Au porphyry deposit, Canadian Cordillera, I: Relationships between PGE, accessory metals and sulfur isotopes in pyrite. Frontiers in Earth Science, 11. <https://www.frontiersin.org/journals/earth-science/articles/10.3389/feart.2023.819129/full>

Colpron, M., 2020. Yukon terranes-A digital atlas of terranes for the northern Cordillera. Yukon Geological Survey. <https://data.geology.gov.yk.ca/Compilation/2#InfoTab>

Cooke, D.R., Hollings, P., and Walshe, J.L., 2005. Giant porphyry deposits: Characteristics, distribution, and tectonic controls. Economic Geology, 100, 801-818.

Cooke, D.R., Wilson, A.J., House, M.J., Wolfe, R.C., Walshe, J.L., Lickfold, V., and Crawford, A.J., 2007. Alkalic porphyry Au-Cu and associated mineral deposits of the Ordovician to Early Silurian Macquarie Arc, New South Wales. Australian Journal of Earth Sciences, 54, 445-463. <https://doi.org/10.1080/08120090601146771>

Grant, D.C., Goudie, D.J., Voisey, C., Shaffer, M., and Sylvester, P., 2018. Discriminating hematite and magnetite via Scanning Electron Microscope-Mineral Liberation Analyzer in the -200 mesh size fraction of iron ores. Applied Earth Science, 127, 30-37. <https://doi.org/10.1080/03717453.2017.1422334>

Gunn, G., 2014. Platinum-group metals. In: Gunn, G., (Ed.), Critical Metals Handbook. John Wiley & Sons, pp. 284-311.

Hall, R.D., and May, B.B., 2013. Geology of the New Afton porphyry copper-gold deposit, Kamloops, British Columbia, Canada. In: Logan, J., and Schroeter, T., (Eds.), Porphyry Systems of Central and Southern BC: Prince George to Princeton. Society of Economic Geologists Field Trip Guidebook 44, pp. 117-128.

Hanley, J., Kerr, M., LeFort, D., Warren, M., MacKenzie, M., and Sedge, C., 2020. Enrichment of platinum-group elements (PGE) in alkalic porphyry Cu-Au deposits in the Canadian Cordillera: New insights from mineralogical and fluid inclusion studies. In: Lang, J.R., Sharman, E.R., and Chapman, J.B., (Eds.), Porphyry Deposits of the Northwestern Cordillera of North America: A 25-Year Update. Canadian Institute of Mining, Metallurgy and Petroleum, Special Volume 57, pp. 88-109.

Hickin, A.S., Ootes, L., Orovan, E.A., Brzozowski, M.J., Northcote, B.K., Rukhlov, A.S., and Bain, W.M., 2024. Critical minerals and mineral systems in British Columbia. In: Geological Fieldwork 2023, British Columbia Ministry of Energy, Mines and Low Carbon Innovation, British Columbia Geological Survey Paper 2024-01, pp. 13-51.

Hofstra, A.H., and Kreiner, D.C., 2020. Systems-deposits-commodities-critical minerals table for the Earth Mapping Resources Initiative (ver. 1.1). U.S. Geological Survey Open File Report 2020-1042, 26 p. <https://doi.org/10.3133/ofr20201042>

Karatas Ahmadli, C., 2025. Platinum-group elements and gold deportment in the Kwanika copper-gold±molybdenum porphyry system, British Columbia, Canada. Unpublished M.Sc. thesis, The University of British Columbia, Vancouver, Canada, 298 p.

Lang, J.R., and Stanley, C.R., 1995a. Contrasting styles of alkalic porphyry Cu-Au deposits in the northern part of the Iron Mask batholith, Kamloops, British Columbia. Canadian Institute of Mining and Metallurgy, Special Volume 46, pp. 581-592.

Lang, J.R., Stanley, C.R., Thompson, J.F.H., and Dunne, K.P., 1995b. Na-K-Ca magmatic-hydrothermal alteration in alkalic porphyry Cu-Au deposits, British Columbia. Mineralogical Association of Canada Short Course 23, pp. 339-366.

LeFort, D., Hanley, J., and Guillong, M., 2011. Subepithermal Au-Pd mineralization associated with an alkalic porphyry Cu-Au deposit, Mount Milligan, Quesnel terrane, British Columbia, Canada. Economic Geology, 106, 781-808. <https://doi.org/10.2113/econgeo.106.5.781>

Lipske, J.L., Wade, D., Hall, R.D., and Petersen, M.A., 2020. Geology and mineralization of the New Afton Cu-Au alkalic porphyry deposit, Kamloops, British Columbia. In: Lang, J.R., Sharman, E.R., and Chapman, J.B., (Eds.), Porphyry Deposits of the Northwestern Cordillera of North America: A 25-Year Update. Canadian Institute of Mining, Metallurgy and Petroleum, Special Volume 57, pp. 648-667.

Lipske, J.L., Wade, D., Hall, R.D., and Petersen, M.A., 2021. Geology and mineralization of the new Afton Cu-Au alkalic porphyry deposits, Kamloops, British Columbia. In: Lang, J.R., Sharman, E.R., and Chapman, J.B., (Eds.), Porphyry Deposits of the Northwestern Cordillera of North America: A 25-Year Update. Canadian Institute of Mining, Metallurgy and Petroleum, Special Volume 57, pp. 648-667.

Logan, J.M., and Mihalynuk, M.G., 2005. Porphyry Cu-Au deposits of the Iron Mask Batholith, southeastern British Columbia. In: Geological Fieldwork 2004, British Columbia Ministry of Energy, Mines and Petroleum Resources, British Columbia Geological Survey Paper 2005-01, pp. 271-290.

Logan, J.M., and Mihalynuk, M.G., 2014. Tectonic Controls on Early Mesozoic Paired Alkaline Porphyry Deposit Belts (Cu-Au Ag-Pt-Pd-Mo) Within the Canadian Cordillera. Economic Geology, 109, 827-858. <https://doi.org/10.2113/econgeo.109.4.827>

Logan, J.M., Mihalynuk, M.G., Ullrich, T.D., and Friedman, R.M., 2006. Geology of the Iron Mask batholith. British Columbia Ministry of Energy, Mines and Petroleum Resources, British Columbia Geological Survey Open File 2006-11, 1:25,000 scale.

Logan, J.M., Mihalynuk, M.G., Ullrich, T., and Friedman, R.M., 2007. U-Pb ages of intrusive rocks and $^{40}Ar/^{39}Ar$ plateau ages of copper-gold-silver mineralization associated with alkaline intrusive centres at Mount Polley and the Iron Mask batholith, southern and central British Columbia. In: Geological Fieldwork 2006, British Columbia Ministry of Energy and Mines, British Columbia Geological Survey Paper 2007-01, pp. 93-116.

MacKenzie, M.K., 2009. Mineralogical controls on the distribution of platinum-group elements and gold in the Afton porphyry deposits, Kamloops, British Columbia. Unpublished B.Sc. thesis, Saint Mary's University, Halifax, Canada, 144 p.

Mihalynuk, M.G., and Diakow, L.J., 2020. Southern Nicola Arc geology (NTS 092H/7NE, 8NW, 9W, 10E, 15E, 16W; 092I/1SW, 2SE). British Columbia Ministry of Energy, Mines and Low Carbon Innovation, British Columbia Geological Survey Geoscience Map 2020-01, 1:50,000 scale.

Mihalynuk, M.G., Diakow, L.J., Friedman, R.M., and Logan, J.M., 2016. Chronology of southern Nicola Arc stratigraphy and deformation. In: Geological Fieldwork 2015, British Columbia Ministry of Energy and Mines, British Columbia Geological Survey Paper 2016-01, pp. 31-63.

Nixon, G.T., 2001. Alkaline-hosted Cu-PGE mineralization in British Columbia: The Whiterocks Mountain plutonic complex, south-central B.C. British Columbia Ministry of Energy and Mines, British Columbia Geological Survey Open File 2001-14, 1:20,000 scale.

Nixon, G.T., 2002. Alkaline hosted Cu-PGE mineralization: The Sappho alkaline plutonic complex, south-central B.C. British Columbia Ministry of Energy and Mines, British Columbia Geological Survey Open File 2002-07, 1:5000 scale.

Nixon, G.T., 2003a. Geological setting of the Lorraine Cu-Au porphyry deposit: New concepts. British Columbia Ministry of Energy and Mines, British Columbia Geological Survey GeoFile 2003-05 (poster).

Nixon, G.T., 2003b. Platinum-group elements in the Afton Cu-Au porphyry deposit, southern British Columbia. In: Geological Fieldwork 2003, British Columbia Ministry of Energy and Mines, British Columbia Geological Survey Paper 2004-01, pp. 263-290.

Nixon, G.T., and Archibald, D.A., 2002. Age of platinum group-element mineralization in the Sappho alkaline complex, south-central British Columbia. In: Geological Fieldwork 2001, British Columbia Ministry of Energy and Mines, British Columbia Geological Survey Paper 2002-01, pp. 171-176.

Nixon, G.T., and Carbono, B., 2001. Whiterocks Mountain alkaline complex, south-central British Columbia: Geology and PGE mineralization. In: Geological Fieldwork 2000, British Columbia Ministry of Energy and Mines, British Columbia Geological Survey Paper 2001-01, pp. 191-222.

Nixon, G.T., and Laflamme, J.H.G., 2002. Cu-PGE mineralization in alkaline plutonic complexes. British Columbia Ministry of Energy and Mines, British Columbia Geological Survey GeoFile 2002-02 (poster).

Nixon, G.T., and Peatfield, G.R., 2003. Geological setting of the Lorraine Cu-Au porphyry deposit, Duckling Creek Syenite Complex, north-central British Columbia. British Columbia Ministry of Energy and Mines, British Columbia Geological Survey Open File 2003-04, 24 p.

Nixon, G.T., Scheel, J.E., Scoates, J.S., Friedman, R.M., Wall, C.J., Gabites, J., and Jackson-Brown, S., 2020. Syn-accretionary multistage assembly of an Early Jurassic Alaskan-type intrusion in the Canadian Cordillera: U-Pb and $^{40}Ar/^{39}Ar$ geochronology of the Turnagain ultramafic-mafic intrusive complex, Yukon-Tanana terrane. Canadian Journal of Earth Sciences, 57, 464-480.

NRCan (Natural Resources Canada), 2024. Canada's critical minerals. <https://www.canada.ca/en/campaign/critical-minerals-in-canada/critical-minerals-an-opportunity-for-canada.html> (last accessed March 2026).

Parsons, J., Wade, D., Katchen, J., and Nadeau-Benoit, V., 2024. NI 43-101 Technical Report on the New Afton Mine, British Columbia, Canada. New Gold Inc., Technical Report, effective date December 31, 2024, 174 p. Available from: <http://sedar.com/>

Pass, H.E., 2010. Breccia-hosted chemical and mineralogical zonation patterns of the northeast zone, Mt. Polley Cu-Ag-Au alkalic porphyry deposit, British Columbia, Canada. Unpublished Ph.D. thesis, University of Tasmania, Hobart, Australia, 286 p. <https://doi.org/10.25959/23210969.v1>

Pass, H.E., Danyushevsky, L., Gilbert, S., Cooke, D.R., and Williams, P.J., 2009. LA-ICP-MS analyses of PGE in pyrite and Cu-sulfides from the Mount Polley alkalic porphyry Cu-Au deposit. In: Smart Science for Exploration and Mining, Proceedings of the 10th Biennial SGA Meeting, Townsville, Australia, pp. 738-740.

Polar, F.A.H.G., 2025. Geology and footprints of porphyry deposits in the Iron Mask District, British Columbia. Unpublished MSc. thesis, University of British Columbia, Vancouver, Canada, 618 p.

Robb, S.J., Boucher, B.M., Mungall, J.E., and Hanley, J.J., 2023. Platinum-group elements (PGE) in the New Afton alkalic Cu-Au porphyry deposit, Canadian Cordillera, II: PGE distribution and models for the hydrothermal coprecipitation of Co-Ni-Pd-Pt in pyrite. Frontiers in Earth Science, 11. <https://doi.org/10.3389/feart.2023.819109>

Rudnick, R.L., and Gao, S., 2014. Composition of the continental crust. In: Treatise on Geochemistry (2nd ed.), Elsevier, pp. 1-64. <https://doi.org/10.1016/B978-0-08-095975-7.00301-6>

Sillitoe, R.H., 2010. Porphyry copper systems. Economic Geology, 105, 3-41.

Sylvester, P.J., 2012. Use of the mineral liberation analyzer (MLA) for mineralogical studies of sediments and sedimentary rocks. In: Sylvester, P., (Ed.), Quantitative Mineralogy and Microanalysis of Sediments and Sedimentary Rocks: Mineralogical Association of Canada Short Course 4, pp. 1-16.

Thompson, J.F.H., Lang, J.R., and Stanley, C.R., 2002. Platinum group elements in alkaline porphyry deposits, British Columbia. In: Exploration and Mining in British Columbia 2001, British Columbia Ministry of Energy and Mines, British Columbia Geological Survey, pp. 57-64.